Structural Requirements for Cellular Uptake and Antisense Activity of Peptide Nucleic Acids Conjugated with Various Peptides†

Yvonne Wolf,*,‡ Stephan Pritz,‡ Saïd Abes,§ Michael Bienert,‡ Bernard Lebleu,§ and Johannes Oehlke‡

Leibniz-Institute of Molecular Pharmacology, Robert-Rössle-Strasse 10, D-13125 Berlin, Germany, and UMR 5124 CNRS, Université Montpellier 2, Place Eugène Bataillon, 34095 Montpellier, France

Received April 10, 2006; Revised Manuscript Received October 6, 2006

ABSTRACT: Peptide nucleic acids (PNAs) have shown great promise as potential antisense drugs; however, poor cellular delivery limits their applications. Improved delivery into mammalian cells and enhanced biological activity of PNAs have been achieved by coupling to cell-penetrating peptides (CPPs). Structural requirements for the shuttling ability of these peptides as well as structural properties of the conjugates such as the linker type and peptide position remained controversial, so far. In the present study an 18mer PNA targeted to the cryptic splice site of a mutated β-globin intron 2, which had been inserted into a luciferase reporter gene coding sequence, was coupled to various peptides. As the peptide lead we used the cell-penetrating α-helical amphipathic peptide KLAL KLAL KAL KAAL KLA-NH_2 [model amphipathic peptide (MAP)] which was varied with respect to charge and structure-forming properties. Furthermore, the linkage and the localization of the attached peptide (C- vs N-terminal) were modified. Positive charge as well as helicity and amphipathicity of the KLA peptide was all required for efficient dose-dependent correction of aberrant splicing. The highest antisense effect was reached within 4 h without any transfection agent. Stably linked conjugates were also efficient in correction of aberrant splicing, suggesting that a cleavable disulfide bond between CPP and PNA is clearly not essential. Moreover, the placement of the attached peptide turned out to be crucial for attaining antisense activity. Coadministration of endosome disrupting agents such as chloroquine or Ca^{2+} significantly increased the splicing correction efficiency of some conjugates, indicating the predominant portion to be sequestered in vesicular compartments.

Peptide nucleic acids (PNAs)[1] have shown great promise as potential antisense drugs since they are potent and metabolically stable RNA- and DNA-binding ligands (*1*). However, cellular delivery remains a limitation as for most nucleic acid-based strategies (*2*). Moreover, uncharged PNAs cannot straightforward be administered by cationic vectors such as polyethylenimine (PEI) or cationic lipids. Complexation with cationic lipids and a DNA carrier is efficient but complicates the approach (*3*). Recently discovered cell-penetrating peptides (CPPs) have gained a lot of attention because of their ability to cross cellular membranes and to transport conjugated cargos, thus possessing great potential for drug delivery (for recent reviews, see refs *4* and *5*). Even though the mechanism of translocation of CPPs is not fully understood yet, a number of promising studies have been published showing enhanced cellular delivery of CPP conjugated with various types of cargo (reviewed in refs *6* and *7*). PNAs covalently attached to simple cationic sequences such as lysine residues have been shown to enter cultured cells efficiently and to affect splicing (*8*−*11*) as well as inhibit gene expression (*12*). Moreover, synthetic peptides such as transportan or model amphipathic peptide (MAP) promoted an enhanced biological activity of PNAs targeted to various intracellular sites (*13*, *14*). Because of the high diversity of these peptides, the structural requirements for the shuttling ability of CPPs are controversial. Additionally, available data may be influenced by the methodology applied for the determination of internalization. CPP−cargo internalization should be evaluated by a reliable biological assay, allowing unequivocal evidence about the delivery of the transported oligonucleotide to its intracellular site of action. Our current study addresses the important question of how the structural properties of PNA−peptide conjugates such as the type of peptide, its placement, and the type of linkage relate to its ability to attain antisense activity evaluated by the splicing-correction assay developed by Kole et al. (*15*). This assay is considered as the most reliable for evaluating

† This work was supported by the European Commission framework 5 (QLK3-CT-2002−01989).

* To whom correspondence should be addressed. Telephone: +49-30-94793240. Fax: +49-30-94793159. E-mail: wolf@fmp-berlin.de.

‡ Leibniz-Institute of Molecular Pharmacology.

§ UMR 5124 CNRS, Université Montpellier 2.

[1] Abbreviations: AEEA, o-linker, 2-[2-(Fmoc-amino)ethoxy]ethoxyacetic acid; CLSM, confocal laser scanning microscopy; CPP, cell-penetrating peptide; DAPI, 4′,6-diamidino-2-phenylindole; DIC, 1,3-diisopropylcarbodiimide; DIPEA, *N*,*N*-diisopropylethylamine; DMEM, Dulbecco's modified Eagle's medium; DMF, *N*,*N*-dimethylformamide; FAM, 5-carboxyfluorescein; FCS, fetal calf serum; Fmoc, *N*-(9-fluorenylmethoxycarbonyl); HATU, *N*-[(dimethylamino)-1*H*-1,2,3-triazolo[4,5-*b*]pyridin-1-ylmethylene]-*N*-methylmethanaminium hexafluorophosphate *N*-oxide; HBTU, *N*-[(1*H*-benzotriazol-1-yl)(dimethylamino)methylene]-*N*-methylmethanaminium hexafluorophosphate *N*-oxide; HOBt, 1-hydroxybenzotriazole; MAP, model amphipathic peptide, KLAL KLAL KAL KAAL KLA-NH_2; MTT, 3-(4,5-dimethylthiazol-2-yl)-2,5-diphenyltetrazolium bromide; NMP, *N*-methylpyrrolidone; PNA, peptide nucleic acid; TCEP, tris(2-carboxyethyl)phosphine; TFA, trifluoroacetic acid; RLU, relative luminescence units.

10.1021/bi0606896 CCC: $33.50
Published on Web 11/18/2006

Table 1: Sequences of PNAs and Peptides Used for Conjugation

	sequence[a]	structural properties[b] and charge
PNA	Ac-C-ooo-cct ctt acc tca gtt aca-ooo-NH_2[c]	
	Ac-ooo-cct ctt acc tca gtt aca-ooo-LPKTGGR-NH_2[d]	
	FAM-ooo-cct ctt acc tca gtt aca-ooo-LPKTGGR-NH_2[d]	
	H-GGG-ooo-cct ctt acc tca gtt aca-ooo-NH_2[d]	
PNA scr	Ac-ooo-tcc ttc cca act ttg aca-ooo-LPKTGGR-NH_2[d]	
	H-GGG-ooo-tcc ttc cca act ttg aca-ooo-NH_2[d]	
KLA	Dns-GC-KLAL KLAL KAL KAAL KLA-NH_2[c]	amphipathic, α-helical, 5+
	H-KLAL KLAL KAL KAAL KLA LPKTGGR-NH_2[d]	
	H-GGG KLAL KLAL KAL KAAL KLA-NH_2[d]	
KGL	Dns-GC-KGLK LKGG LGL LGKL KLG-NH_2[c]	unstructured, 5+
	H-KGLK LKGG LGL LGKL KLG LPKTGGR-NH_2[d]	
KAL	Dns-GC-KALK LKAA LAL LAKL KLA-NH_2[c]	nonamphipathic, α-helical, 5+
	H-KALK LKAA LAL LAKL KLA LPKTGGR-NH_2[d]	
ELA	Dns-GC-ELAL ELAL EAL EAAL ELA-NH_2[c]	amphipathic, α-helical, 5−
	H-ELAL ELAL EAL EAAL ELA LPKTGGR-NH_2[d]	
	H-GGG ELAL ELAL EAL EAAL ELA-NH_2[d]	
RLA	Dns-GC-RLAL RLAL RAL RAAL RLA-NH_2[c]	amphipathic, α-helical, 5+
	H-RLAL RLAL RAL RAAL RLA LPKTGGR-NH_2[d]	
Pen	Dns-GC-RQI KIW FQN RRM KWK K-NH_2[c]	poor α-helical amphipathic, 7+
	H-RQI KIW FQN RRM KWK KLPKTGGR-NH_2[d]	
	H-GGG RQI KIW FQN RRM KWK K-NH_2[d]	

[a] Key: lower case letters = PNA bases; upper case letters = amino acids; Dns = dansyl; FAM = 5-carboxyfluorescein; o = ethylene glycol spacer. [b] According to CD measurements in 50% trifluoroethanol (TFE) in water (*46*). [c] Used for disulfide coupling. [d] Used for sortase-mediated ligation.

the nuclear delivery of steric blocking oligonucleotide analogues since it is a positive read-out assay and only the appearance of a specific oligonucleotide within the nucleus of a viable cell will allow correct splicing. In brief, the coding sequence of a luciferase reporter gene is interrupted by a mutated β-globin intron 2 (IVS2−705) carrying a cryptic splice site. This mutation causes aberrant splicing of luciferase pre-mRNA and therefore prevents translation of luciferase. However, masking the cryptic splice site by steric blocking oligonucleotide analogues induces correct splicing, restoring luciferase expression. In the present study an 18mer PNA (cct ctt acc tca gtt aca) targeted to the cryptic splice site was covalently attached to various peptides. As the peptide lead, we used the cell-penetrating α-helical amphipathic peptide KLAL KLAL KAL KAAL KLA-NH_2, also known as model amphipathic peptide (MAP) (*16*, *17*), which was varied with respect to structure-forming properties and charge (Table 1). Additionally, we investigated the well-known cell-penetrating peptide penetratin (*18*). As the conjugation approach, disulfide coupling was performed, which is a commonly used method for the assembly of peptide−cargo conjugates. The disulfide bond is thought to be cleaved rapidly once within the reducing environment of the cell. However, it is not yet clear whether the use of biolabile bonds such as a disulfide bridge offers advantages or may be essential for attaining antisense activity. Therefore, a series of conjugates with stable linkages was synthesized by a sortase-mediated ligation approach (*19*). Moreover, the localization of the peptide (C- vs N-terminal) was modified since influences of the attached peptide on the biological activity of oligonucleotide conjugates have been occasionally reported (*20*, *21*). In order to contribute to the elucidation of the mechanism of internalization, we also investigated the influence of the known lysosomotropic agent chloroquine (*22*, *23*) as well as Ca^{2+} (*24*, *25*) on the ability of the conjugates to correct aberrant splicing.

EXPERIMENTAL PROCEDURES

General. Chemicals and reagents were purchased from Sigma (Deisenhof, Germany) or Bachem (Heidelberg, Germany) unless specified otherwise.

Synthesis of PNAs, Peptides, and PNA−Peptide Conjugates. (A) PNA and Peptide Solid-Phase Synthesis. PNAs were synthesized manually by Fmoc [*N*-(9-fluorenylmethoxycarbonyl)] chemistry (*26*, *27*). Fmoc (Bhoc) PNA monomers were purchased from Applied Biosystems and used at 0.5 M dissolved in *N*-methylpyrrolidone (NMP). Before and after PNA assembly six AEEA spacers [o-linker, 2-[2-(Fmoc-amino)ethoxy]ethoxyacetic acid; Fluka], three at the C-terminus and three at the N-terminus, were coupled to a TentaGel S RAM resin (0.22 mmol/g; Rapp) in the same manner as the PNA monomers. For the sortase-mediated ligation (*19*) either a LPKTGGR motif or a triglycine had to be inserted before or after PNA assembly, respectively (sequences of the PNAs are shown in Table 1). The amino groups were deprotected by 20% piperidine in *N*,*N*-dimethylformamide (DMF) for 6 min. After five washes with DMF the monomers were coupled to the resin by *N*-[(dimethylamino)-1*H*-1,2,3-triazolo[4,5-*b*]pyridin-1-ylmethylene]-*N*-methylmethanaminium hexafluorophosphate *N*-oxide (HATU, 0.45 M) in DMF and 5 equiv of *N*,*N*-diisopropylethylamine (DIPEA) and *sym*-collidine (2,4,6-trimethylpyridine) for 20 min. A double coupling was performed. The resin was washed five times with DMF after each coupling step. A capping step followed using 4% acetic anhydride and 4% DIPEA in DMF. Then the resin was split into two portions. To one portion a Cys (StBu) residue was attached at the N-terminus for disulfide coupling; to the other portion a triglycine was coupled for the sortase-mediated ligation. In order to obtain 5-carboxyfluorescein- (FAM-) labeled PNAs, the Fmoc-deprotected resin was treated with 5 equiv of 5-carboxyfluorescein (FAM), 1-hydroxybenzotriazole (HOBt, 5 equiv), and 1,3-diisopropylcarbodiimide (DIC, 4.8 equiv) in DMF for at least 24 h. The coupling of FAM was repeated

twice. The N-terminal Fmoc group was removed before final cleavage. Finally, the product was cleaved from the resin by 20% *m*-cresol in trifluoroacetic acid (TFA). PNAs were purified and analyzed by RP-HPLC on a PolyEncap A300 column with eluent A, 0.1% TFA in water, and eluent B, 80% acetonitrile in 0.1% TFA (gradient: 5−95% B in 45 min), and monitoring at 260 nm. MALDI-TOF mass spectrometry was performed on a Voyager DE STR workstation using a matrix of α-cyanohydroxycinnamic acid (5 mg/mL) in 60% acetonitrile/0.3% TFA and provided the expected $[M + H]^+$. The sequences of the PNAs are shown in Table 1.

Peptides were synthesized automatically on a 433A peptide synthesizer (Applied Biosystems) by the solid-phase method using standard Fmoc chemistry. Syntheses were carried out on TentaGel S RAM resin (0.22 mmol/g; Rapp) using N^{α}-Fmoc-protected amino acid derivatives (5 equiv, 0.5 M) and *N*-[(1*H*-benzotriazol-1-yl)(dimethylamino)methylene]-*N*-methylmethanaminium hexafluorophosphate *N*-oxide (HBTU, 4.9 equiv, 0.5 M) as coupling reagent in the presence of DIPEA (10 equiv, 2.0 M) in DMF. Double couplings for 20 min were allowed to proceed; N-terminal deblocking was carried out twice with 20% piperidine in DMF for 5 min. All washes were made with DMF. Final cleavage from the resin and deprotection of side chain functionalities were achieved by a mixture of 5% phenol, 2% triisopropylsilane, and 5% water in TFA for 2 h. Purification and characterization were carried out as described for PNAs. For the sortase-mediated ligation peptide sequences were elongated with either a LPKTGGR motif or a triglycine at the C- or N-terminus, respectively. Peptides used were either KLA, also known as model amphipathic peptide (MAP), which is a positively charged, α-helical amphipathic peptide, ELA, wherein the lysine residues are replaced by glutamic acid, KGL, which is an unstructured peptide moiety, KAL, an nonamphipathic analogue of KLA, RLA, which is even more basic than KLA due to the replacement of the lysine residues by arginines, or penetratin. The sequences of all synthesized peptides are shown in Table 1.

(B) Assembly of the Disulfide-Linked PNA−Peptide Conjugates. (1) Activation of the PNA with 2,2′-Dithiodipyridine. To remove the protecting group (StBu) from the cysteine residue to a solution of PNA (sequence is shown in Table 1; 1 mg dissolved in 200 μL of ammonium bicarbonate buffer, pH 9.0), 250 μL of β-mercaptoethanol was added, and the reaction mixture was left to stand for 1 h at room temperature. Then the PNA was precipitated with ether. To the precipitate, isolated by centrifugation, was added a solution of tris(2-carboxyethyl)phosphine (TCEP, 0.5 mg/mL in ammonium acetate buffer, pH 7.0) to cleave probably generated PNA dimers into monomers. The reaction mixture was kept for 30 min at 50 °C. Next, a solution of 2,2′-dithiodipyridine (10 mg/mL in ammonium acetate buffer, pH 7.0) was added, and the reaction mixture was left to stand for 3 h at 50 °C. The product was precipitated with ether and dissolved in ammonium acetate buffer, pH 7.0.

(2) Formation of the Disulfide Bond. To a solution of 10 nmol of the activated PNA in ammonium acetate buffer (pH 7.0) was added a 5-fold excess of the peptide. In the case of the MAP-derived peptides (KLA, RLA, ELA) acetonitrile (1:1 v/v) had to be added to the reaction mixture to prevent precipitation. The reaction mixture was kept for 30−45 min at 50 °C. Purification and analysis of the conjugates were carried out on an analytical PolyEncap C18 column (heated at 50 °C) using a gradient of 5−95% eluent B in 45 min (eluent A, 0.1% TFA in water; eluent B, 80% acetonitrile in 0.1% TFA). Detection was performed at 260 and 220 nm, respectively. The lyophilized products were dissolved in 0.1% TFA and stored in the freezer. MALDI-TOF mass spectrometry was performed on a Voyager DE STR workstation using a matrix of α-cyanohydroxycinnamic acid (5 mg/mL) in 60% acetonitrile/0.3% TFA and provided the expected $[M + H]^+$.

(C) Assembly of PNA−Peptide Conjugates with Stable Linkages. The syntheses of the stably linked PNA−peptide conjugates were carried out using a sortase-mediated ligation strategy (*19*). The detailed procedure will be reported elsewhere (S. Pritz, in preparation). In brief, ligations were carried out in aqueous buffered solutions containing 50 mM Tris-HCl, 150 mM NaCl, and 5 mM $CaCl_2$ at pH 7.5. Solutions (600 μL) containing 1.66 mM CPP, 0.33 mM PNA, and 6 μM sortase were dialyzed against 1 L of the aqueous buffer (mentioned above) for 24 h at ambient temperature through a membrane with a molecular mass cutoff of 2000 Da. Purification of these conjugates was carried out on a semipreparative PolyEncap C18 column (heated at 50 °C) using a gradient of 10−80% eluent B in 70 min (eluent A, 0.1% TFA in water; eluent B, 80% acetonitrile in 0.1% TFA; flow rate, 4 mL/min) and monitoring at 220 nm. The appropriate fractions were lyophilized and analyzed by analytical HPLC and MALDI-TOF mass spectrometry as described above. Conjugates of KLA with a scrambled sequence of the PNA (KLA−PNA scr and PNA−KLA scr, respectively) were synthesized to assess the sequence specificity of the antisense effect. For the synthesis of FAM-labeled PNA conjugates with KLA, ELA, and penetratin, a PNA labeled with 5-carboxyfluorescein (FAM) at the N-terminus was used to enable fluorescence microscopy studies.

Cell Culture. HeLa pLuc 705 cells were cultured in Dulbecco's modified Eagle's medium (DMEM) containing 4.5 g/L glucose (Gibco) supplemented with 10% (v/v) fetal calf serum (FCS) and 1% (v/v) nonessential amino acids in a humidified atmosphere containing 5% CO_2.

Splicing Correction Assay. For assessing the splicing correction, HeLa pLuc 705 cells were plated in 96-well plates at a density of 2×10^4 cells per well and cultured overnight. The culture medium was discarded, and the cells were washed twice with PBS. The cells were incubated for 4 h either with the naked PNA or with the PNA−peptide conjugates at various concentrations diluted in OptiMEM. Incubation was continued for another 20 h in DMEM containing 10% FCS. For chloroquine and Ca^{2+} experiments conjugates were prepared at 1 μM in OptiMEM containing 100 μM chloroquine and 6 mM $CaCl_2$, respectively, and added to the cells for 4 h incubation. After the cells were washed, incubation was continued for another 20 h in DMEM/10% FCS. In the case of chloroquine and Ca^{2+} treatment the growth medium was supplemented with 100 μM chloroquine or 6 mM $CaCl_2$, respectively. After 24 h cells were washed twice with PBS and lysed with the reporter lysis buffer (Promega). The plates were stored at −80 °C for at least 4 h to ensure complete lysis. Luciferase activity was quantified by using the luciferase assay system from Promega and measuring the luminescence by a GENios Pro

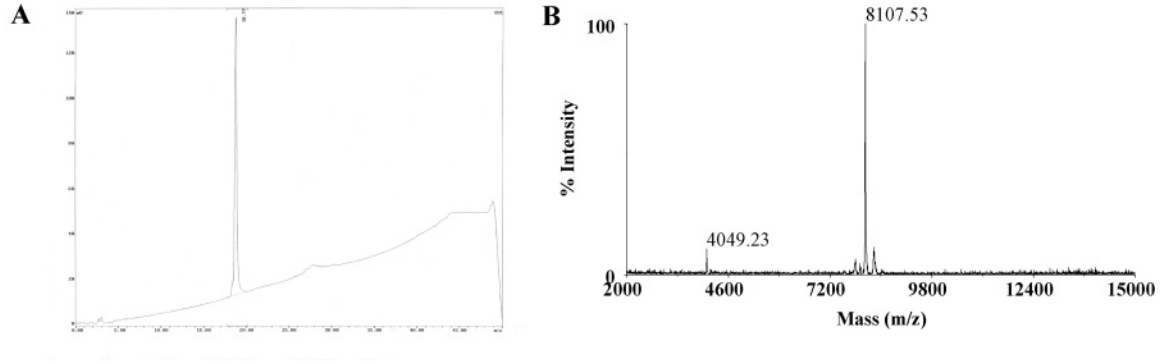

C

conjugate	sequence	mw calculated	mw found
KLA-PNA	H-KLAL KLAL KAL KAAL KLA LPKTGGG ooo-cct ctt acc tca gtt aca-ooo-NH_2	8106.7	8107.5
PNA-KLA	Ac-ooo-cct ctt acc tca gtt aca-ooo-LPKTGGG KLAL KLAL KAL KAAL KLA-NH_2	8148.7	8150.6
FAM-PNA-KLA	FAM-ooo-cct ctt acc tca gtt aca-ooo-LPKTGGG KLAL KLAL KAL KAAL KLA-NH_2	8464.9	8472.9
KLA-PNA scr	H-KLAL KLAL KAL KAAL KLA LPKTGGG ooo-tcc ttc cca act ttg aca-ooo-NH_2	8106.7	8104.3
PNA-KLA scr	Ac-ooo-tcc ttc cca act ttg aca-ooo-LPKTGGG KLAL KLAL KAL KAAL KLA-NH_2	8148.7	8149.6
KGL-PNA	H-KGLK LKGG LGL LGKL KLG LPKTGGG ooo-cct ctt acc tca gtt aca-ooo-NH_2	8022.5	8026.0
KAL-PNA	H-KALK LKAA LAL LAKL KLA LPKTGGG ooo-cct ctt acc tca gtt aca-ooo-NH_2	8106.7	8107.0
ELA-PNA	H-ELAL ELAL EAL EAAL ELA LPKTGGG ooo-cct ctt acc tca gtt aca-ooo-NH_2	8111.4	8112.7
PNA-ELA	Ac-ooo-cct ctt acc tca gtt aca-ooo-LPKTGGG ELAL ELAL EAL EAAL ELA-NH_2	8153.4	8155.1
FAM-PNA-ELA	FAM-ooo-cct ctt acc tca gtt aca-ooo-LPKTGGG ELAL ELAL EAL EAAL ELA-NH_2	8469.7	8475.4
RLA-PNA	H-RLAL RLAL RAL RAAL RLA LPKTGGG ooo-cct ctt acc tca gtt aca-ooo-NH_2	8246.7	8253.3
Pen-PNA	H-RQI KIW FQN RRM KWK KLPKTGGG ooo-cct ctt acc tca gtt aca-ooo-NH_2	8475.9	8471.7
PNA-Pen	Ac-ooo-cct ctt acc tca gtt aca-ooo-LPKTGGG RQI KIW FQN RRM KWK K-NH_2	8518.0	8515.7
FAM-PNA-Pen	FAM-ooo-cct ctt acc tca gtt aca-ooo-LPKTGGG RQI KIW FQN RRM KWK K-NH_2	8834.2	8835.6

FIGURE 1: Analytical data of the stably linked conjugates. HPLC chromatogram (A) and MALDI-TOF mass spectrum (B) of KLA−PNA. (C) Calculated and found molecular masses of all stably linked conjugates.

luminometer (Tecan). Total cellular protein quantities were measured by Bradford protein assay according to the manufacturer's protocol and read using a Safire plate reader (Tecan) at a wavelength of 595 nm. Data were expressed as relative luminescence units (RLU) per microgram of protein. Each data point is the average of the three replicates. Cell viability was assessed using the MTT [3-(4,5-dimethylthiazol-2-yl)-2,5-diphenyltetrazolium bromide] assay.

Confocal Laser Scanning Microscopy Studies. For confocal microscopy studies HeLa pLuc 705 cells (10^5/well) were plated on coverslips and cultured in growth medium overnight. The medium was discarded, and the cells were washed with PBS followed by incubation with the conjugates at 1 μM in 500 μL of OptiMEM for 4 h. In the case of chloroquine or Ca^{2+} treatment the incubation solution was supplemented with either 100 μM chloroquine or 6 mM Ca^{2+}. Then the cells were washed two times with PBS and cultured for another 20 h in DMEM/10% FCS, in the case of chloroquine or Ca^{2+} treatment supplemented with 100 μM chloroquine or 6 mM Ca^{2+}, respectively. CLSM measurement was performed using a LSM 510 invert confocal laser scanning microscope (Carl Zeiss Jena GmbH, Jena, Germany; software, LSM 510 META image examiner, version 3.2, Carl Zeiss Jena GmbH, Jena, Germany). Nuclei were stained with 1 μg/mL DAPI (4′,6-diamidino-2-phenylindole; Sigma-Aldrich, Germany) (*28*). Subsequent to the observation, the viability of the cells was assessed by Trypan Blue staining. Excitation was performed at 488 nm (FAM), 345 nm (DAPI), and 543 nm (Trypan Blue), and emission was measured at 515, 455, and 570 nm, respectively.

RESULTS

Synthesis of Disulfide and Stably Linked PNA−Peptide Conjugates. PNA−peptide conjugates were designed to test the influence of the attached peptides on the antisense activity and cellular uptake of PNAs. The PNA sequence (shown in Table 1) was flanked by three ethylene glycol spacers (o-linker) at each side to increase solubility and minimize aggregation of the PNA−peptide conjugates. The sequences of the PNA−peptide conjugates synthesized by the sortase-mediated ligation approach are shown in Figure 1 (panel C). These conjugates carry a LPKTGGG motif between the peptide and the PNA which was required for the enzyme (sortase) recognition. Panels A and B of Figure 1 show a

A

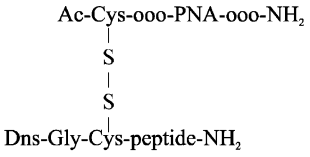

B

conjugate	mw calculated	mw found
PNA-SS-KLA	8049.6	8053.4
PNA-SS-KGL	7965.5	7961.9
PNA-SS-KAL	8049.6	8049.6
PNA-SS-ELA	8054.4	8050.5
PNA-SS-RLA	8189.7	8195.9
PNA-SS-Pen	8418.9	8415.5

FIGURE 2: Analytical data of the disulfide-linked conjugates. (A) Structure of disulfide-linked conjugates. The linkage is in all cases between the N-terminus of the PNA and the N-terminus of the peptides. (B) Calculated and found molecular masses of all disulfide-linked conjugates.

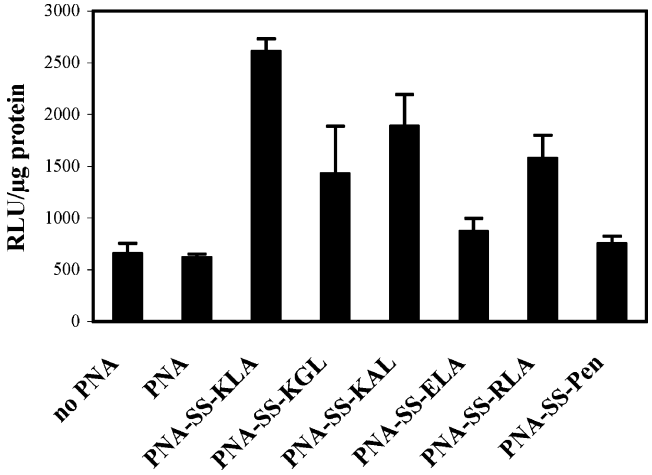

FIGURE 3: Splicing correction of the disulfide-linked PNA−peptide conjugates. HeLa pLuc 705 cells were incubated in OptiMEM in the absence of PNA (no PNA) or in the presence of 1 μM naked PNA or various disulfide-linked PNA−peptide conjugates for 4 h. Luciferase expression was analyzed 24 h later and expressed in relative luminescence units (RLU)/μg of protein. Each experiment was done in triplicate, and error bars are indicated.

HPLC chromatogram and a mass spectrum of the stably linked KLA−PNA conjugate. In all cases purity was >95%. MALDI-TOF mass spectrometry provided the correct mass for all conjugates (Figure 1, panel C).

The structure of the disulfide-bridged conjugates is displayed in Figure 2 (panel A); in each case the Cys residue is located at the N-terminus of the peptide. Precipitation of the MAP-derived peptide conjugates was reduced by adding acetonitrile to the reaction mixture and heating it at 50 °C. Purification of the disulfide-linked conjugates was also carried out by reverse-phase HPLC, and characterization was performed by MALDI-TOF mass spectrometry, providing the correct mass for the conjugates (Figure 2, panel B).

Helicity, Amphipathicity, and Positive Charge of the Peptides Attached to the PNA Are Requested for Promoting an Efficient Splicing Correction. We investigated the ability of the PNA−peptide constructs in correction of aberrant splicing using HeLa pLuc 705 cells which carry a mutated luciferase gene (*15*). As shown in Figure 3 in the case of the unconjugated PNA there was no significant increase of luciferase luminescence. Conjugation of the PNA with the cationic, α-helical amphipathic peptide KLA via a disulfide bond (PNA−SS−KLA) led at 1 μM to a 5-fold enhanced

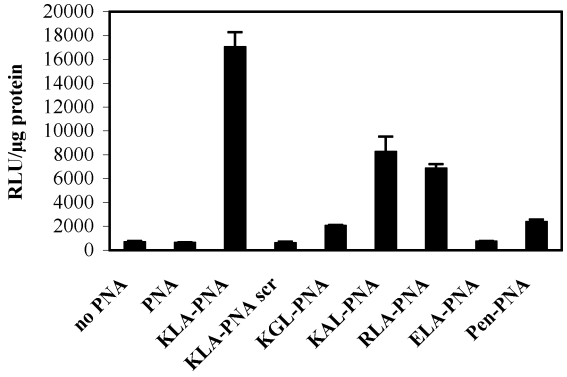

FIGURE 4: Splicing correction of the stably linked PNA−peptide conjugates. HeLa pLuc 705 cells were incubated in OptiMEM in the absence of PNA (no PNA) or in the presence of 1 μM naked PNA or various stably linked PNA−peptide conjugates for 4 h. Luciferase expression was analyzed 24 h later and expressed in relative luminescence units (RLU)/μg of protein. Each experiment was done in triplicate, and error bars are indicated.

biological activity compared to the naked PNA. The corresponding unstructured KGL (PNA−SS−KGL) and nonamphipathic KAL (PNA−SS−KAL) constructs were less effective (2.3-fold and 3-fold, respectively) in correction of splicing than KLA. For PNAs conjugated to the negatively charged ELA (PNA−SS−ELA) wherein the lysine residues have been replaced by glutamic acid and surprisingly for PNA attached to the well-known cell-penetrating peptide penetratin (PNA−SS−Pen), no activity could be observed. It has been repeatedly reported that peptides containing arginine residues are better taken up by cells (*29*−*31*) and thus are more potent than lysine analogues (*32*). Therefore, we also tested a PNA conjugate with a KLA analogue wherein the lysine residues have been replaced by arginines (PNA−SS−RLA). Interestingly, this modification did not lead to a higher antisense effect than the lysine derivative.

A Cleavable Disulfide Bond, Allowing the Release of the PNA Oligomer, Is Not Required To Restore Aberrant Splicing. Next, we addressed the issue whether a linker as a disulfide bridge, which is expected to be cleaved rapidly once within the reducing environment of the cell, is advantageous or essential for achieving antisense activity. Interestingly, as shown in Figure 4 the stable conjugates were also effective in correction of splicing, suggesting a cleavable disulfide bridge not to be essential for attaining antisense activity. For the stably linked conjugates derived from the MAP peptide moiety a similar pattern to that obtained for the disulfide-linked conjugates was found. Highest luciferase activity was observed for the PNA conjugated with KLA (KLA−PNA), possessing cationic as well as α-helical amphipathic properties, followed by those with the nonamphipathic KAL (KAL−PNA) and highly basic RLA peptides (RLA−PNA). The constructs with the unstructured KGL (KGL−PNA) and penetratin (Pen−PNA), respectively, showed a slightly enhanced antisense activity. No effect was observed for the negatively charged ELA−PNA. The sequence specificity of the effect was ascertained by the inactivity of a conjugate of KLA with a scrambled PNA sequence (KLA−PNA scr). In order to find out whether the LPKTGGG motif, which was required for the synthesis of the stably linked conjugates by the sortase-mediated ligation approach, has an influence on cellular uptake and antisense activity, a stably linked KLA−PNA conjugate (H-KLALKLALKALKAALKLAoooc-

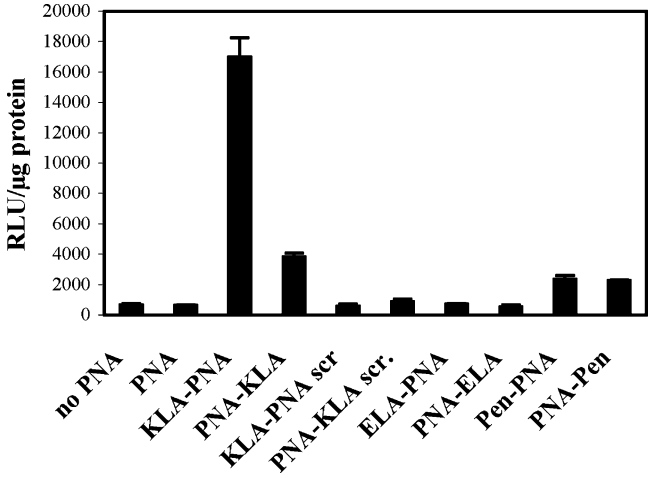

FIGURE 5: Influence of the position of the peptide attached to the PNA on the splicing correction of the conjugates. HeLa pLuc 705 cells were incubated in OptiMEM in the absence of PNA (no PNA) or in the presence of 1 μM naked PNA or various stably linked PNA−peptide conjugates for 4 h. Luciferase expression was analyzed 24 h later and expressed in relative luminescence units (RLU)/μg of protein. Each experiment was done in triplicate, and error bars are indicated.

ctcttacctcagttacaooo-NH_2) lacking this motif was synthesized by straightforward solid-phase synthesis. Antisense activity of this conjugate in Kole's splicing-correction assay was found to be comparable with the KLA−PNA construct carrying the LPKTGGG sequence (data not shown). Moreover, the six ethylene glycol spacers (o-linker) which were inserted to increase solubility and minimize aggregation did not influence the biological activity since a KLA−PNA conjugate (H-KLALKLALKALKAALKLAcctcttacctcagttaca-NH_2) showed similar correction of aberrant splicing as the one used in this study containing six o-spacers (data not shown).

The Position of the Peptide Attached to the PNA Influences the Antisense Efficiency of the Conjugates. Considering the orientation of the peptide attached to the PNA (C- vs N-terminal), the conjugate bearing the KLA peptide moiety at the C-terminus of the PNA (PNA−KLA) was much less effective in splicing correction than the analogue coupled to the N-terminus of the PNA (KLA−PNA) as shown in Figure 5. In case of the penetratin conjugates Pen−PNA (coupled to the N-terminus of the PNA) and PNA−Pen (attached to the C-terminus), no significant difference in antisense activity could be observed. The negatively charged ELA peptide, no matter if attached to the N- or C-terminus of the PNA, did not promote any antisense activity of the PNA. The scrambled PNAs conjugated to KLA (KLA−PNA scr, PNA−KLA scr) did not show any biological activity, confirming the sequence specificity of the obtained effects. These results clearly demonstrate that a cleavable disulfide bond between CPP and PNA is not essential for biological activity. However, the orientation of the coupling (C- vs N-terminal) seems to have an impact on achieving activity. As shown in Figures 6 and 7, respectively, the ability of the KLA conjugates (PNA−SS−KLA, KLA−PNA, and PNA−KLA) to correct aberrant splicing exhibited a strong dependence on the incubation concentration and time. The naked PNA did not show any activity up to 2.5 μM. The antisense effect of KGL and KAL conjugates was only slightly enhanced at higher concentrations (up to 2.5 μM) (data not

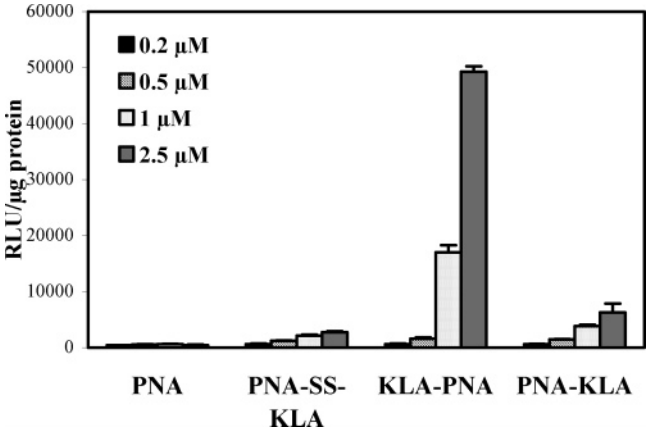

FIGURE 6: Concentration dependence of splicing correction. HeLa pLuc 705 cells were incubated in OptiMEM with 0.2 (black bars), 0.5 (striped bars), 1 (dotted bars), or 2.5 μM (gray bars) naked PNA or various PNA−KLA conjugates (PNA−SS−KLA, KLA−PNA, and PNA−KLA, respectively) for 4 h. Data are expressed in relative luminescence units (RLU)/μg of protein.

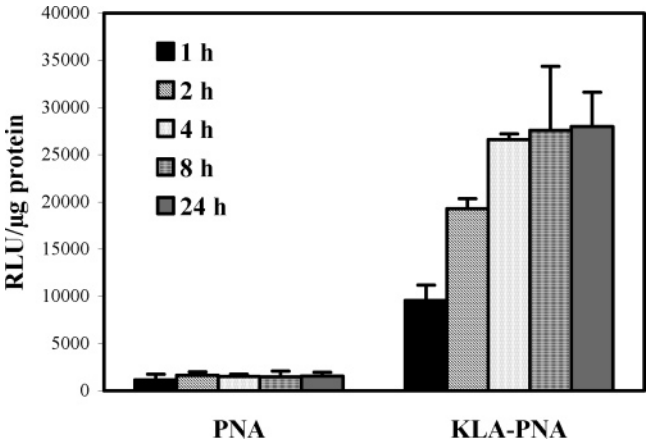

FIGURE 7: Time−course experiment. Splicing correction of 1 μM naked PNA or KLA−PNA incubated for 1, 2, 4, 8, or 24 h, respectively, with HeLa pLuc 705 cells. Luciferase expression was analyzed 24 h later and expressed in relative luminescence units (RLU)/μg of protein.

shown). One should note that MAP-derived PNA conjugates showed rather high cytotoxicity at higher concentrations (20% cell viability at 4 μM; data not shown) assessed by the MTT assay. The maximum of luciferase activity of the stable KLA−PNA construct was reached within 4 h, the time point at which the set of data in Figures 3−6 and 8 was taken. There was no significant increase in luciferase activity after incubating the cells for 8 and 24 h, respectively. We also tested the influence of serum on the splicing correction. The presence of serum had no impact on the splicing activity (data not shown).

The Antisense Effect of the Conjugates Is Enhanced by Lysosomotropic Agents. It has been repeatedly reported that agents, known to mediate a release from endosomes, could significantly enhance the antisense activity of oligonucleotide− and PNA−CPP conjugates (*11*, *33*). The most commonly used pharmacological agent for such purpose is chloroquine (*22*, *23*). Similar effects were observed after addition of 6 mM Ca^{2+} (*24*, *32*). In order to gain insight into the mechanism of the delivery of PNA−peptide conjugates used in this study, we also investigated the antisense activity in the presence of chloroquine (100 μM)

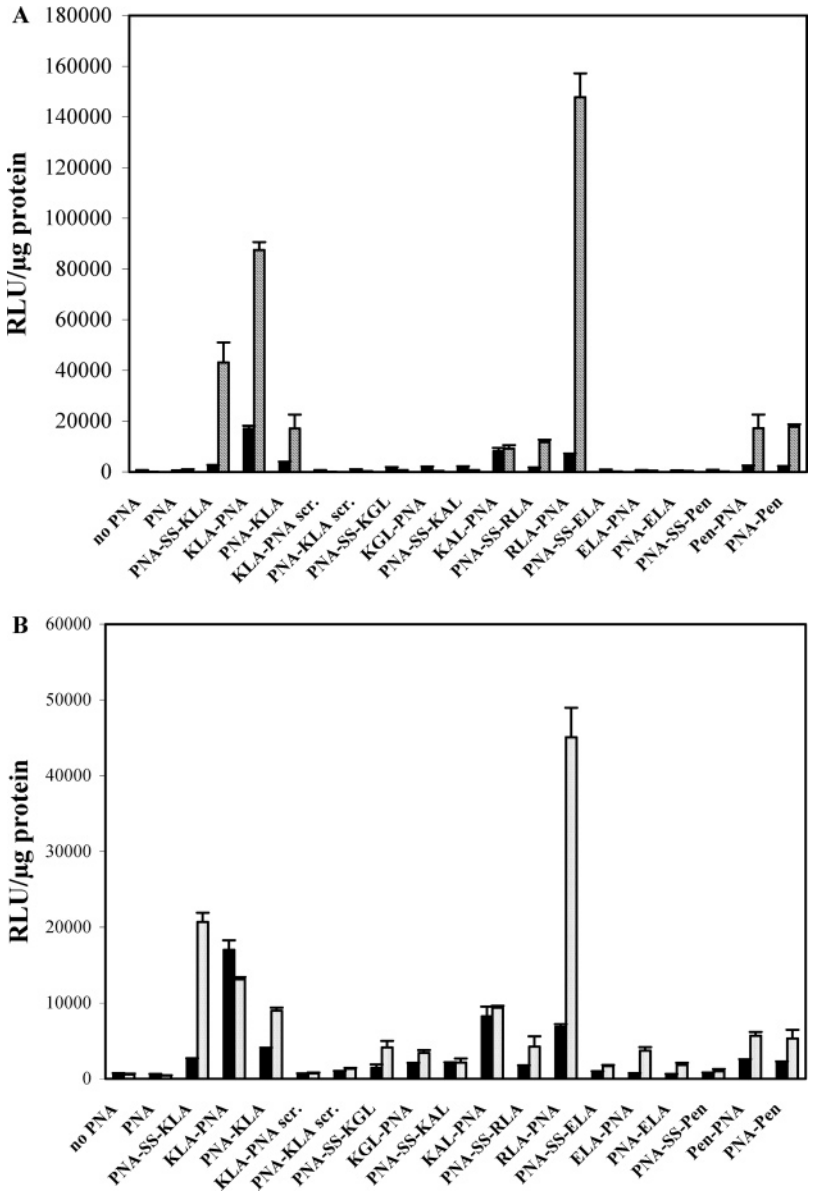

FIGURE 8: Effect of lysosomotropic agents on the splicing correction of the conjugates. (A) Chloroquine treatment. HeLa pLuc 705 cells were incubated in the absence of PNA (no PNA) or in the presence of 1 μM naked PNA and various PNA−peptide conjugates without (black bars) or with 100 μM chloroquine (striped bars) for 4 h. Cells were then grown in DMEM/10% FCS, in the case of chloroquine treatment containing 100 μM chloroquine, for a further 20 h. Data are expressed in relative luminescence units (RLU)/μg of protein. Experiments have been done in triplicate. Error bars are indicated. (B) Ca^{2+} treatment. HeLa pLuc 705 cells were incubated in the absence of PNA (no PNA) or in the presence of 1 μM naked PNA and various PNA−peptide conjugates without (black bars) or with 6 mM $CaCl_2$ (dotted bars) for 4 h. Cells were then grown in DMEM/10% FCS, in case of calcium treatment supplemented with 6 mM $CaCl_2$, for 20 h. Data are expressed in relative luminescence units (RLU)/μg of protein. Error bars are indicated.

and Ca^{2+} (6 mM). In a first set of experiments 100 μM chloroquine was coadministered with the conjugates and has been left on the cells for 4 h. No significant difference in splicing correction could be observed (data not shown). However, when chloroquine (100 μM) has been supplemented to the medium containing 10% FCS as a posttreatment and left in total on the cells for 24 h, tremendous effects became apparent for the amphipathic KLA peptide disulfide-linked to the PNA (PNA−SS−KLA) and stably linked at the N-terminus of the PNA (KLA−PNA) (47- and 96-fold, respectively, related to the naked PNA) (Figure 8, panel A). An even greater enhancement (162-fold) was found for the RLA−PNA, the arginine analogue of KLA. The stably linked conjugates of penetratin (Pen−PNA and PNA−Pen) as well as PNA−KLA revealed only slightly enhanced antisense activities. No significant enhancement in biological activity was observed for the naked PNA and conjugates with other peptides such as KGL, ELA, and KAL. Coadministration of chloroquine had no influence on the sequence specificity since scrambled PNAs attached to KLA (KLA−PNA scr, PNA−KLA scr) remained ineffective in splicing correction. Moreover, chloroquine treatment did not affect the cell viability assessed by the MTT test (data not shown). These data infer a rather huge amount at least of some conjugates (PNA−SS−KLA, KLA−PNA, and RLA−PNA) to be sequestered in vesicular compartments.

A slightly different pattern to that obtained with chloroquine treatment could be observed after co-incubation with 6 mM Ca^{2+} (Figure 8, panel B). A great enhancement of the biological effect was seen again for the stably linked

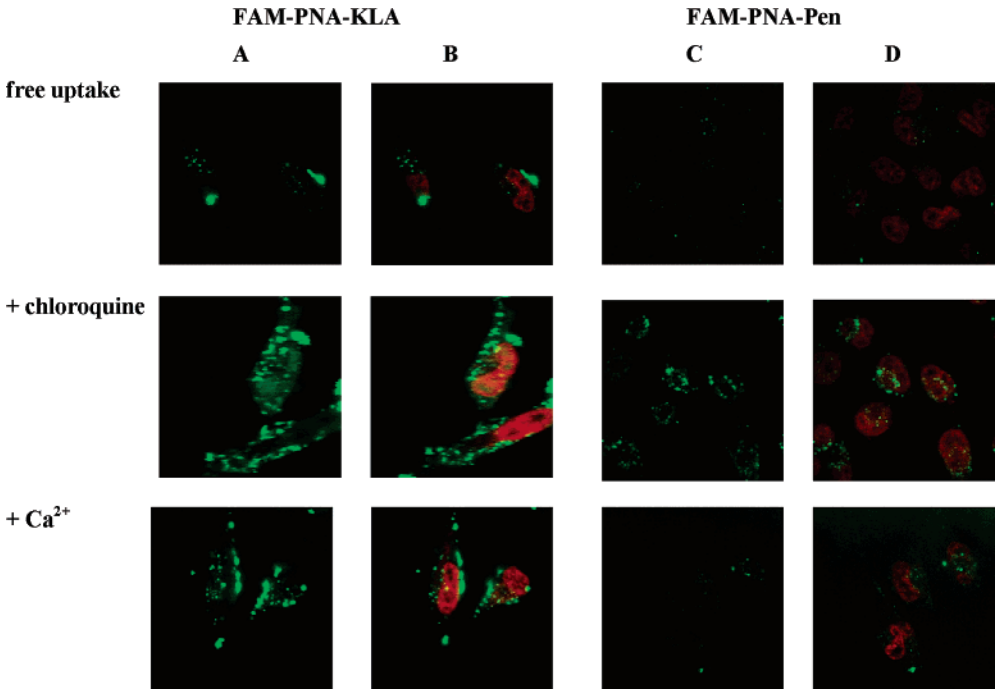

FIGURE 9: Confocal microscopy studies. Confocal microscopy images of the uptake of FAM-labeled, stably linked PNA−CPP conjugates when incubated for 4 h at 1 μM in the absence and presence of lysosomotropic agents. Cells were then cultured for another 20 h in DMEM/10% FCS, in the case of chloroquine or Ca^{2+} treatment supplemented with 100 μM chloroquine or 6 mM Ca^{2+}, respectively. Nuclei are stained red with DAPI. (For DAPI a pseudocolor is used.) In green color (A and C) fluorescein fluorescence is shown. (B) and (D) are overlaid images of DAPI staining (red color) and fluorescein fluorescence (green color). Colocalization can be seen in yellow. The first line represents the internalization without any lysosomotropic agents (free uptake) while the second and third lines show images of the uptake in the presence of chloroquine or Ca^{2+}, respectively.

RLA−PNA conjugate. However, for the stably linked KLA−PNA no enhancement of luciferase activity was found in the presence of Ca^{2+} whereas the activity of PNA−SS−KLA and PNA−KLA showing little splicing correction in the absence of chloroquine or Ca^{2+} did increase. In context, our data suggest more complex factors additionally to sequestration within and release from endosomes to influence the splicing correction activity of the conjugates and the action of chloroquine and Ca^{2+}.

Indication of Endosomal Release by Confocal Microscopy in the Presence of Chloroquine. To obtain visual evidence for conjugate release from endosomal compartments by adding chloroquine (100 μM) or Ca^{2+} (6 mM), we performed confocal microscopy of FAM-labeled PNAs conjugated with KLA, ELA, and penetratin (PNA−KLA, PNA−ELA, PNA−Pen) in the absence and presence of these reagents. Only live, nonfixed cells were used to prevent artifacts caused by cell fixation (*34*). To facilitate visualization of any nuclear uptake, DAPI (4′,6-diamidino-2-phenylindole) was used to stain the cell nucleus. By using the same experimental setup as taken for the antisense activity experiments, we were unable to detect any uptake for the naked PNA and the negatively charged PNA−ELA (data not shown). In the absence of lysosomotropic agents PNA−KLA and PNA−Pen showed a punctate fluorescence (Figure 9, first line, panels A−D) in the cytosol, suggesting endosomal sequestration. However, the PNA conjugated with KLA (Figure 9, first line, panels A and B) showed higher uptake and a quite different distribution compared to the PNA−Pen conjugated, being concentrated in large aggregates at the cell membrane (accumulation was observed within 5 min) as well as inside the cytoplasm. By analyzing the internalization by the CLSM software (*35*), significant nuclear uptake was detected for PNA−KLA whereas the PNA conjugated to penetratin could not be seen inside the nucleus, which is consistent with the lack of activity in the splicing-correction assay. Coadministration of chloroquine led to significant nuclear uptake of both conjugates. The PNA−KLA conjugate (second line, panels A and B) appeared diffusively distributed whereas the PNA−Pen (second line, panels C and D) showed a punctate fluorescence within the nucleus. Addition of 6 mM Ca^{2+} resulted in an enhanced accumulation of the PNA−KLA conjugate (Figure 9, third line, panels A and B) at the cell membrane, outside as well as inside the cell, as large aggregates, with a few spots being located within the nucleus. The effect of Ca^{2+} on the distribution of the PNA−Pen conjugate (Figure 9, third line, panels C and D) was less strong compared to that of chloroquine. Overall, the confocal microscopy data provide evidence for sequestration of a dominant part of PNA−CPP conjugates in endosomes.

DISCUSSION

The current study addresses important questions about structural properties of PNA−peptide conjugates requested for attaining antisense activity such as the peptide sequence, its placement, and the type of linkage. Our data clearly demonstrate that nuclear delivery and antisense activity of PNAs can be enhanced by the attachment of cell-penetrating peptides. The KLA−PNA conjugates, possessing cationic as well as α-helical amphipathic properties, showed highest nuclear activity in Kole's splicing-correction assay (*15*). This effect was dose- as well as time-dependent. It has been repeatedly reported that replacement of lysine by arginine residues resulted in an increased cellular uptake as well as biological activity (*29*−*32*). Probably this is due to the ability of the guanidinium group of arginine to form hydrogen bonds

with sulfate, phosphate, and carboxylate groups in the membrane (*36*, *37*), thereby producing less polar ion pair complexes capable of diffusing into the membrane (*36*). As demonstrated in this study, replacement of the lysine residues of the KLA peptide by arginines (RLA) did not lead to a higher antisense activity of the corresponding PNA conjugate. We assume that the guanidinium side chain which seems to be preferred for simple basic peptide sequences such as oligoarginines (e.g., Arg_9) is less important for the KLA peptide, and other structural properties such as amphipathicity and helicity also seem to contribute to cellular uptake and biological activity. Indeed, conjugates of peptides lacking amphipathicity or helicity (KAL and KGL, respectively) were less effective in restoring aberrant splicing. Conjugation of the PNA with a negatively charged peptide, ELA, did not lead to any enhanced biological effect. These data, which are consistent with reports of others (*12*, *21*, *38*), indicate that structure requirements such as positive charge and amphipathicity, being regarded to be characteristic of cell-penetrating peptides (*5*, *39*, *40*), seem to be essential for attaining an enhanced antisense activity of corresponding PNA−peptide conjugates. The important question whether the intracellular release of the PNA by cleavage of the linkage of the conjugate is advantageous or even essential for biological activity remained unresolved so far. In the present study we gained clear evidence that a disulfide bond between the peptide and the PNA which is expected to be rapidly cleaved within the cell is not essential for biological activity. This is in line with our recent studies showing equal antisense activity of a disulfide- and an amide-bound PNA−KLA conjugate targeted to the nociceptin/orphanin FQ receptor of spontaneously beating neonatal rat cardiomyocytes (*14*), (Y. Wolf, submitted for publication). In the current study the stably linked conjugates showed an even higher antisense activity than the disulfide-bridged ones (Figures 3 and 4). Even though the additional LPKTGGG motif of the stably linked conjugates, which had to be inserted into the conjugate sequence for enzymatic ligation, had no significant impact on the antisense activity, we cannot exclude that other structural differences of the conjugates (positioning of PNA to peptide sequence) also contribute to their activity, and further investigations are needed.

We observed a tremendous decrease of the antisense effect when the peptide has been attached to the C-terminus of the PNA (Figure 5), suggesting the position of the peptide (C- vs N-terminal) to play an important role for the biological activity of the conjugates. Even though the PNA−KLA conjugate has been efficiently delivered into the nucleus after endosomal release by chloroquine treatment (Figure 9), the antisense activity was only little increased (Figure 8, panel A). These data indicate that, apparently, the N-terminus of the PNA is the preferred attachment site for the peptides, which might be understood in terms of PNA−RNA binding. Indeed, PNAs modify mRNA processing by steric blocking (*41*). Recently, Moulton et al. also observed a dramatic decrease of antisense activity of a phosphorodiamidate morpholino oligomer (PMO) when cationic peptides or bulky moieties such as carboxyfluorescein or cholesterol had been coupled to the 3′-end of the oligos (*20*). The authors hypothesized steric interferences of the PMO−RNA binding to be the reason for this phenomenon. In order to gain insight into the role of the peptide attached to the PNA and its position, studies on the binding affinity of PNA−peptide conjugates to the target sequence using the surface plasmon resonance technique are currently under way.

Overall, however, peptide features such as positive charge and amphipathicity seem not to be sufficient to promote biological activity of PNAs. Indeed, there are also examples of PNA conjugates with well-known CPPs such as penetratin, as shown in our study, or Tat (*32*, *33*) being inactive. The lack of activity seems not to be due to cellular uptake since an enhanced internalization into HeLa cells for a PNA attached to penetratin has been detected by means of CE-LIF in our recent study (Y. Wolf, submitted for publication) being in line with others (*42*, *43*). This is also consistent with our confocal microscopy data presented in the current study revealing efficient uptake into HeLa cells for PNA−KLA as well as PNA−Pen conjugates. One of the reasons for the absence of activity could be that only a minor portion of the conjugates is internalized by a nonendocytic pathway formerly regarded to be characteristic of CPPs (*39*, *40*) while the predominant portion is taken up by endocytosis and remains sequestered within endosomal compartments. It has recently been reported that endosome destabilization by lysosomotropic agents (*11*, *32*) or fusogenic peptides such as, for instance, hemagglutinin peptide (*44*) led to enhanced biological effects of CPP−cargo conjugates. In order to gain insight into mechanistic aspects of the intracellular delivery of the PNA−peptide conjugates evaluated in the current study, we also investigated the antisense activity in the presence of the lysosomotropic agent chloroquine as well as Ca^{2+}. Treatment with chloroquine has shown great effect on the ability of some peptide conjugates to restore correct splicing (Figure 7, panel A). In contrast to the experiments conducted without chloroquine the stably linked RLA−PNA conjugate, wherein the lysine residues had been replaced by arginine, became more efficient than its lysine analogue KLA after addition of chloroquine or Ca^{2+}. A modulation of the target affinity of the PNA caused by the cationic peptides might be the reason for this enhanced activity. Without chloroquine assistance the RLA conjugate seems to be sequestered in endosomes and therefore less active in splicing correction compared to the KLA−PNA conjugate which might more efficiently escape the endosomes itself. Furthermore, nonendocytotic pathways are possibly involved in the uptake of the KLA−PNA conjugate being in line with our previous CE-LIF studies (*14*) (Y. Wolf, submitted for publication). This has also been recently discussed by Shiraishi et al. (*45*), who observed an antisense activity in Kole's model for a stably linked KLA−PNA conjugate. The antisense activity could even be enhanced by photochemical treatment facilitating endosomal release. We gained clear evidence for conjugate release from endosomes and enhanced nuclear uptake by confocal microscopy for the FAM-labeled stably linked PNA−KLA conjugate when chloroquine was coadministered. However, for the PNA−KLA there was only a little enhancement of splicing activity after chloroquine treatment while the antisense activity of the KLA−PNA conjugate has dramatically increased. This supports the assumption that the peptide attached at the C-terminus of the PNA might hinder the binding of the PNA to its target probably due to steric interferences. In contrast to the diffused chloroquine-induced distribution, Ca^{2+} seems more to stimulate the accumulation of the PNA−KLA at the cell mem-

brane. Therefore, the mechanism of the Ca^{2+} effect to increase the splicing activity seems to be more complex and cannot be simply explained an increased endosomal release. These observations are consistent with those of Shiraishi et al. (*32*), who found an enhanced antisense activity in Kole's splicing model for $(Arg)_9$−PNA and Tat−PNA conjugates in the presence of Ca^{2+}. Overall, these data indicate that there is no direct correlation between uptake and antisense activity, suggesting other factors (e.g., the binding affinity to intracellular targets) also to be crucial for attaining biological activity. Therefore, our current work is focused on binding studies of PNAs linked to various peptides using the surface plasmon resonance technique.

ACKNOWLEDGMENT

We thank D. Krause, B. Pisarz, and H. Lerch for excellent technical assistance. Burkhard Wiesner is thanked for support with the confocal microscopy studies.

REFERENCES

1. Egholm, M., Buchardt, O., Christensen, L., Behrens, C., Freier, S. M., Driver, D. A., Berg, R. H., Kim, S. K., Norden, B., and Nielsen, P. E. (1993) PNA hybridizes to complementary oligonucleotides obeying the Watson-Crick hydrogen-bonding rules, *Nature 365*, 566−568.
2. Pooga, M., Land, T., Bartfai, T., and Langel, U. (2001) PNA oligomers as tools for specific modulation of gene expression, *Biomol. Eng. 17*, 183−192.
3. Hamilton, S. E., Simmons, C. G., Kathiriya, I. S., and Corey, D. R. (1999) Cellular delivery of peptide nucleic acids and inhibition of human telomerase, *Chem. Biol. 6*, 343−351.
4. Vives, E. (2005) Present and future of cell-penetrating peptide mediated delivery systems: "is the Trojan horse too wild to go only to Troy?", *J. Control Release 109*, 77−85.
5. Zorko, M., and Langel, U. (2005) Cell-penetrating peptides: mechanism and kinetics of cargo delivery, *Adv. Drug Deliv. Rev. 57*, 529−545.
6. Gait, M. J. (2003) Peptide-mediated cellular delivery of antisense oligonucleotides and their analogues, *Cell. Mol. Life Sci. 60*, 844−853.
7. Lochmann, D., Jauk, E., and Zimmer, A. (2004) Drug delivery of oligonucleotides by peptides, *Eur. J. Pharm. Biopharm. 58*, 237−251.
8. Sazani, P., Kang, S. H., Maier, M. A., Wei, C. F., Dillman, J., Summerton, J., Manoharan, M., and Kole, R. (2001) Nuclear antisense effects of neutral, anionic and cationic oligonucleotide analogs, *Nucleic Acids Res. 29*, 3965−3974.
9. Sazani, P., Gemignani, F., Kang, S. H., Maier, M. A., Manoharan, M., Persmark, M., Bortner, D., and Kole, R. (2002) Systemically delivered antisense oligomers upregulate gene expression in mouse tissues, *Nat. Biotechnol. 20*, 1228−1233.
10. Siwkowski, A. M., Malik, L., Esau, C. C., Maier, M. A., Wancewicz, E. V., Albertshofer, K., Monia, B. P., Bennett, C. F., and Eldrup, A. B. (2004) Identification and functional validation of PNAs that inhibit murine CD40 expression by redirection of splicing, *Nucleic Acids Res. 32*, 2695−2706.
11. Abes, S., Williams, D., Prevot, P., Thierry, A., Gait, M. J., and Lebleu, B. (2006) Endosome trapping limits the efficiency of splicing correction by PNA-oligolysine conjugates, *J. Control Release 110*, 595−604.
12. Kaihatsu, K., Huffman, K. E., and Corey, D. R. (2004) Intracellular uptake and inhibition of gene expression by PNAs and PNA-peptide conjugates, *Biochemistry 43*, 14340−14347.
13. Pooga, M., Soomets, U., Hallbrink, M., Valkna, A., Saar, K., Rezaei, K., Kahl, U., Hao, J. X., Xu, X. J., WiesenfeldHallin, Z., Hokfelt, T., Bartfai, A., and Langel, U. (1998) Cell penetrating PNA constructs regulate galanin receptor levels and modify pain transmission in vivo, *Nat. Biotechnol. 16*, 857−861.
14. Oehlke, J., Wallukat, G., Wolf, Y., Ehrlich, A., Wiesner, B., Berger, H., and Bienert, M. (2004) Enhancement of intracellular concentration and biological activity of PNA after conjugation with a cell-penetrating synthetic model peptide, *Eur. J. Biochem. 271*, 3043−3049.
15. Kang, S. H., Cho, M. J., and Kole, R. (1998) Up-regulation of luciferase gene expression with antisense oligonucleotides: Implications and applications in functional assay developments, *Biochemistry 37*, 6235−6239.
16. Oehlke, J., Scheller, A., Wiesner, B., Krause, E., Beyermann, M., Klauschenz, E., Melzig, M., and Bienert, M. (1998) Cellular uptake of an alpha-helical amphipathic model peptide with the potential to deliver polar compounds into the cell interior non-endocytically, *Biochim. Biophys. Acta 1414*, 127−139.
17. Oehlke, J., Lorenz, D., Wiesner, B., and Bienert, M. (2005) Studies on the cellular uptake of substance P and lysine-rich, KLA-derived model peptides, *J. Mol. Recognit. 18*, 50−59.
18. Derossi, D., Joliot, A. H., Chassaing, G., and Prochiantz, A. (1994) The third helix of the Antennapedia homeodomain translocates through biological membranes, *J. Biol. Chem. 269*, 10444−10450.
19. Mao, H. Y., Hart, S. A., Schink, A., and Pollok, B. A. (2004) Sortase-mediated protein ligation: A new method for protein engineering, *J. Am. Chem. Soc. 126*, 2670−2671.
20. Moulton, H. M., Nelson, M. H., Hatlevig, S. A., Reddy, M. T., and Iversen, P. L. (2004) Cellular uptake of antisense morpholino oligomers conjugated to arginine-rich peptides, *Bioconjugate Chem. 15*, 290−299.
21. Albertshofer, K., Siwkowski, A. M., Wancewicz, E. V., Esau, C. C., Watanabe, T., Nishihara, K. C., Kinberger, G. A., Malik, L., Eldrup, A. B., Manoharan, M., Geary, R. S., Monia, B. P., Swayze, E. E., Griffey, R. H., Bennett, C. F., and Maier, M. A. (2005) Structure-activity relationship study on a simple cationic peptide motif for cellular delivery of antisense peptide nucleic acid, *J. Med. Chem. 48*, 6741−6749.
22. Midoux, P., Mendes, C., Legrand, A., Raimond, J., Mayer, R., Monsigny, M., and Roche, A. C. (1993) Specific gene transfer mediated by lactosylated poly-L-lysine into hepatoma cells, *Nucleic Acids Res. 21*, 871−878.
23. Erbacher, P., Roche, A. C., Monsigny, M., and Midoux, P. (1996) Putative role of chloroquine in gene transfer into a human hepatoma cell line by DNA/lactosylated polylysine complexes, *Exp. Cell Res. 225*, 186−194.
24. Haberland, A., Knaus, T., Zaitsev, S. V., Stahn, R., Mistry, A. R., Coutelle, C., Haller, H., and Bottger, M. (1999) Calcium ions as efficient cofactor of polycation-mediated gene transfer, *Biochim. Biophys. Acta 1445*, 21−30.
25. Zaitsev, S., Buchwalow, I., Haberland, A., Tkachuk, S., Zaitseva, I., Haller, H., and Bottger, M. (2002) Histone H1-mediated transfection: role of calcium in the cellular uptake and intracellular fate of H1-DNA complexes, *Acta Histochem. 104*, 85−92.
26. Thomson, S. A., Josey, J. A., Cadilla, R., Gaul, M. D., Hassman, C. F., Luzzio, M. J., Pipe, A. J., Reed, K. L., Ricca, D. J., Wiethe, R. W., and Noble, S. A. (1995) Fmoc mediated synthesis of peptide nucleic-acids, *Tetrahedron 51*, 6179−6194.
27. Braasch, D. A., and Corey, D. R. (2001) Synthesis, analysis, purification, and intracellular delivery of peptide nucleic acids, *Methods 23*, 97−107.
28. Kapuscinski, J., and Szer, W. (1979) Interactions of 4′,6-diamidine-2-phenylindole with synthetic polynucleotides, *Nucleic Acids Res. 6*, 3519−3534.
29. Futaki, S., Suzuki, T., Ohashi, W., Yagami, T., Tanaka, S., Ueda, K., and Sugiura, Y. (2001) Arginine-rich peptides−An abundant source of membrane-permeable peptides having potential as carriers for intracellular protein delivery, *J. Biol. Chem. 276*, 5836−5840.
30. Mitchell, D. J., Kim, D. T., Steinman, L., Fathman, C. G., and Rothbard, J. B. (2000) Polyarginine enters cells more efficiently than other polycationic homopolymers, *J. Pept. Res. 56*, 318−325.
31. Rothbard, J. B., Garlington, S., Lin, Q., Kirschberg, T., Kreider, E., McGrane, P. L., Wender, P. A., and Khavari, P. A. (2000) Conjugation of arginine oligomers to cyclosporin A facilitates topical delivery and inhibition of inflammation, *Nat. Med. 6*, 1253−1257.
32. Shiraishi, T., Pankratova, S., and Nielsen, P. E. (2005) Calcium ions effectively enhance the effect of antisense peptide nucleic acids conjugated to cationic tat and oligoarginine peptides, *Chem. Biol. 12*, 923−929.
33. Turner, J. J., Ivanova, G. D., Verbeure, B., Williams, D., Arzumanov, A. A., Abes, S., Lebleu, B., and Gait, M. J. (2005) Cell-penetrating peptide conjugates of peptide nucleic acids (PNA)

as inhibitors of HIV-1 Tat-dependent trans-activation in cells, *Nucleic Acids Res. 33*, 6837−6849.
34. Richard, J. P., Melikov, K., Vives, E., Ramos, C., Verbeure, B., Gait, M. J., Chernomordik, L. V., and Lebleu, B. (2003) Cell-penetrating peptides. A reevaluation of the mechanism of cellular uptake, *J. Biol. Chem. 278*, 585−590.
35. Wiesner, B., Lorenz, D., Krause, E., Beyermann, M., and Bienert, M. (2002) Measurement of intracellular fluorescence in the presence of a strong extracellular fluorescence using confocal laser scanning microscopy, *LAMSO 3*, 1−17.
36. Sakai, N., and Matile, S. (2003) Anion-mediated transfer of polyarginine across liquid and bilayer membranes, *J. Am. Chem. Soc. 125*, 14348−14356.
37. Salvatella, X., Martinell, M., Gairi, M., Mateu, M. G., Feliz, M., Hamilton, A. D., de Mendoza, J., and Giralt, E. (2004) A tetraguanidinium ligand binds to the surface of the tetramerization domain of protein P53, *Angew. Chem., Int. Ed Engl. 43*, 196−198.
38. Tripathi, S., Chaubey, B., Ganguly, S., Harris, D., Casale, R. A., and Pandey, V. N. (2005) Anti-HIV-1 activity of anti-TAR polyamide nucleic acid conjugated with various membrane transducing peptides, *Nucleic Acids Res. 33*, 4345−4356.
39. Lindgren, M., Hällbrink, M., Prochiantz, A., and Langel, Ü. (2000) Cell-penetrating peptides, *Trends Pharmacol. Sci.* 21, 99−103.
40. Langel, Ü. Ed. (2002) Cell-penetrating peptides, *Handbook of Cell-Penetrating Peptides*, CRC Press LLC, Boca Raton, FL.
41. Braasch, D. A., and Corey, D. R. (2002) Novel antisense and peptide nucleic acid strategies for controlling gene expression, *Biochemistry 41*, 4503−4510.
42. Simmons, C. G., Pitts, A. E., Mayfield, L. D., Shay, J. W., and Corey, D. R. (1997) Synthesis and membrane permeability of PNA-peptide conjugates, *Bioorg. Med. Chem. Lett. 7*, 3001−3006.
43. Koppelhus, U., Awasthi, S. K., Zachar, V., Holst, H. U., Ebbesen, P., and Nielsen, P. E. (2002) Cell-dependent differential cellular uptake of PNA, peptides, and PNA-peptide conjugates, *Antisense Nucleic Acid Drug Dev. 12*, 51−63.
44. Wadia, J. S., Stan, R. V., and Dowdy, S. F. (2004) Transducible TAT-HA fusogenic peptide enhances escape of TAT-fusion proteins after lipid raft macropinocytosis, *Nat. Med. 10*, 310−315.
45. Shiraishi, T., and Nielsen, P. E. (2006) Photochemically enhanced cellular delivery of cell penetrating peptide-PNA conjugates, *FEBS Lett. 580*, 1451−1456.
46. Scheller, A., Oehlke, J., Wiesner, B., Dathe, M., Krause, E., Beyermann, M., Melzig, M., and Bienert, M. (1999) Structural requirements for cellular uptake of alpha-helical amphipathic peptides, *J. Pept. Sci. 5*, 185−194.

BI0606896